RESEARCH ARTICLE

# Hydroquinone Exposure Induces Organ-Specific Antioxidant Alterations and Histopathological Injury in the Liver, Kidney, Lung, and Spleen of Maternal Mice

Nur Afizah Yusoff[1], Isna Syafiqa Isnimuddin[1], Nurizzati Arifah Mazlan[1], Nurul Husnina Khairul Zain[1], Sukyna Elhosain Dadali Abdula[1], Siti Balkis Budin[1], Izatus Shima Taib[1], Nur Najmi Mohamad Anuar[2], Nor Malia Abd Warif[2], Zariyantey Abd Hamid[1,*]

[1]Biomedical Science Programme, Centre for Diagnostic, Therapeutic and Investigative Studies, Faculty of Health Sciences, Universiti Kebangsaan Malaysia, Jalan Raja Muda Abdul Aziz, Kuala Lumpur 50300, Malaysia
[2]Biomedical Science Programme, Centre for Toxicology and Health Risk Studies, Faculty of Health Sciences, Universiti Kebangsaan Malaysia, Jalan Raja Muda Abdul Aziz, Kuala Lumpur 50300, Malaysia

*Corresponding author. Email: zyantey@ukm.edu.my

Received date: Aug 26, 2026; Revised date: Oct 12, 2026; Accepted date: Oct 19, 2026

## Abstract

**BACKGROUND:** Gestational benzene exposure is associated with oxidative stress and fetal toxicity. However, data regarding the organ specificity of oxidative and histopathological injury in maternal tissues during gestation remains widely unexplored. Therefore, this study was conducted to evaluate oxidative damage and histopathological alterations in the liver, kidney, lung, and spleen following maternal benzene exposure.

**METHODS:** Eighteen pregnant ICR mice (8-10 weeks, 30-40 g) were randomly divided into three groups (n=6/each): healthy mice as control, mice that was given hydroquinone (HQ) orally at 25 mg/kg (HQ25) and 50 mg/kg (HQ50) on gestational day-12, -14, and -16. On gestational day-18, mice were sacrificed and the liver, kidney, lung, and spleen harvested for analysis. Malondialdehyde (MDA), advanced oxidation protein products (AOPP), glutathione (GSH), and superoxide dismutase (SOD) activity were analyzed by measuring thiobarbituric acid-reactive substances (TBARS), oxidation of potassium iodide (KI), 5,5′-dithiobis(2-nitrobenzoic acid) (DTNB), and nitroblue tetrazolium (NBT), respectively. Histopathological analysis was performed using hematoxylin and eosin (H&E) staining.

**RESULTS:** No significant changes in oxidative stress markers were observed in the organs of HQ-treated groups compared with control group. However, a significant reduction in GSH levels ($p$=0.02) was detected in the spleen of HQ50 group, while SOD activity ($p$=0.01) was significantly reduced in the lungs of both HQ-treated groups compared with the control group. Histopathological examination of the HQ-treated groups revealed hepatocyte necrosis in the liver; altered glomerular size, enlarged Bowman's space, increased cellularity, thickening of Bowman's capsule, and degeneration of the proximal tubular brush border in the kidneys; lymphocyte aggregation and increased cellularity in the spleen; and irregular bronchial walls, inflammatory cell infiltration, enlarged alveoli, and epithelial damage in the lungs.

**CONCLUSION:** HQ exposure induced organ-specific antioxidant alterations and histopathological injury across maternal organs, suggesting differential maternal organ responses to gestational HQ exposure despite unremarkable oxidative damage.

**KEYWORDS:** benzene, hydroquinone, maternal toxicity, oxidative stress, histopathology

***Indones Biomed J. 2026; 18(5): 449-60***

## Introduction

The body possesses sophisticated defence mechanisms to counteract oxidative stress through endogenous and exogenous antioxidants. Yet, excessive oxidative stress induced by environmental pollutants, poor dietary habits, and chronic diseases can overwhelm these protective systems. Benzene ($C_6H_6$), a major environmental and occupational pollutant, is well known for its carcinogenic



Copyright © 2026 The Prodia Education and Research Institute.
This work is licensed under a Creative Commons Attribution-NonCommercial 4.0 International (CC-BY-NC) License.

and hematotoxic effects in humans.(1) Because benzene is widely used as an industrial solvent, exposure is common in industries such as shoe manufacturing, petrochemical processing, and fuel stations. At the same time, smoking remains a major source among the general population.(1) Classified as a Group 1 carcinogen by the International Agency for Research on Cancer (IARC), benzene has been strongly linked to aplastic anemia and leukemia in both prenatal and adult exposures.(2,3) Its toxic effects arise from metabolic biotransformation in the liver, mediated by cytochrome P450 enzymes, particularly CYP2E1, which generate reactive metabolites such as hydroquinone (HQ).(4)

HQ is considered one of the most toxic metabolites of benzene. Several metabolites undergo redox cycling, producing reactive oxygen species (ROS) such as superoxide anions, hydrogen peroxide ($H_2O_2$), and hydroxyl radicals. Excessive ROS can overwhelm antioxidant defences, damaging deoxyribonucleic acid (DNA), lipids, and proteins, and impairing cellular function.(5) Oxidative stress has been implicated in pregnancy complications and developmental disorders.(6,7) Pregnancy itself involves extensive anatomical and metabolic adaptations that alter maternal redox homeostasis. Elevated oxygen utilization and basal metabolic activity increase ROS production, while enhanced fatty acid metabolism during the second trimester further promotes oxidative processes. In the third trimester, insulin resistance and lipid catabolism contribute to additional $H_2O_2$ accumulation.(6) These physiological changes heighten maternal vulnerability to oxidative insults, including those from benzene-derived HQ.

Such vulnerability places maternal organs under considerable stress. For example, the kidneys, essential for fluid and metabolic homeostasis, are particularly susceptible due to their high mitochondrial content and ROS generation through respiration and nicotinamide adenine dinucleotide phosphate (NADPH) oxidase activity.(8) Similarly, the lungs, continuously exposed to oxygen and pollutants, express multiple ROS-generating enzymes, making them prone to oxidative injury following HQ exposure.(9) Disruption of pulmonary homeostasis during pregnancy may compromise maternal respiratory function and potentially alter the intrauterine environment. The spleen, central to hematological balance and immune function, is also at risk. Occupational studies have shown reduced white and red blood cell counts in benzene-exposed workers, underscoring its hematotoxic potential.(10) These findings highlight the importance of investigating effects of HQ on splenic tissue and hematopoietic function during pregnancy.

Collectively, existing evidence indicates that HQ poses significant health concerns, particularly during pregnancy, when physiological and metabolic adaptations may alter susceptibility to toxic insults. Although benzene and HQ toxicity has been extensively investigated, much of the existing evidence on organ toxicity has been derived from non-gestational models or individual-organ assessments, while gestational studies have predominantly focused on fetal toxicity, inclusive of placental, developmental, or hematopoietic outcomes. Consequently, comparative multi-organ responses in maternal during gestational HQ exposure remain insufficiently characterized. To address this knowledge gap, the present study simultaneously evaluated oxidative stress and antioxidant status along with histopathological alterations across four vital organs in maternal, inclusive of liver, kidney, lung, and spleen, following oral HQ exposure during gestation. By providing organ-specific insights via a gestational-exposure model, this work advances understanding of differential maternal organ susceptibility to HQ toxicity during pregnancy. Although maternal toxicity during pregnancy may have implications for fetal well-being, fetal and placental parameters were not assessed in the present study; therefore, the findings are limited to maternal organ toxicity and should not be interpreted as direct evidence of fetal or placental effects. Further investigation integrating maternal, placental, and fetal outcomes is warranted to clarify the broader systemic and developmental consequences of gestational HQ exposure.

## Methods

### Experimental Animals and Mating Procedures

A total of 27 Imprinting Control Region (ICR) mice, aged 8-10 weeks and weighing 30-40 g, were used in this experimental study, comprising 9 males and 18 females. All 18 females were mated and subsequently included as confirmed pregnant mice in the experimental study. These mice were obtained from the Animal Resource Unit, Kuala Lumpur, Malaysia. Prior to experimentation, the animals were assessed to ensure that they were in good general health, as indicated by clean and well-groomed fur, active movement, and normal behaviour. Pregnant or lactating females, as well as animals of either sex that developed illness or died during the study, were excluded from the experimental procedures. The mice were housed under controlled environmental conditions at 22±2°C and 55% relative humidity, with a 12-hour light/dark cycle, and were

provided *ad libitum* access to standard laboratory chow and drinking water. The animals were acclimatized to the housing conditions for 7 days before commencement of the experiment. All experimental procedures were conducted at the Animal House, Kuala Lumpur, Malaysia, following the ethically approved protocol. For mating, two fertile female mice identified as being in the estrus phase were housed overnight with one male. Successful mating was identified by the presence of a copulation plug and the detection of sperm in vaginal smears examined the following morning microscopically. The day on which sperm was detected was individually designated as gestational day (GD)-0 for each female, ensuring that all pregnant mice entered the treatment phase at the same GD-12. Pregnancy progression was subsequently monitored until GD-18 based on progressive maternal body-weight gain and observable physical changes associated with pregnancy, as previously described.(11)

**Experimental Design**

Confirmed pregnant ICR mice (n=18) were housed individually in separate cages, with each mouse serving as the experimental unit. The sample size was determined using the Resource Equation Approach described previously. (12) The pregnant mice were randomly assigned to three experimental groups (n=6 per group): a control group receiving distilled water, a low-dose group (HQ25) receiving 25 mg/kg HQ, and a high-dose group (HQ50) receiving 50 mg/kg HQ. Maternal body weight was recorded daily throughout the experimental period, from GD-0 to GD-18. To evaluate dose-dependent effects while minimizing potential lethality, HQ with 98% purity (Cat. No. G144531; Sigma-Aldrich, St. Louis, MO, USA) was administered via oral gavage on GD-12, -14, and -16.(13) These gestational time points were chosen to target mid-gestation, a critical developmental period characterized by increased oxidative stress and substantial changes in hematopoietic and immune system activity, which may increase cellular susceptibility to xenobiotic-induced stress.(14) On GD-18, shortly before the expected onset of parturition, all pregnant mice were euthanized via intraperitoneal administration of a ketamine and xylazine anesthetic cocktails. The liver, kidneys, lungs, and spleens were subsequently harvested for assessment of HQ-induced oxidative stress and histopathological alterations across multiple maternal organs.

**Multi-organ Tissue Collection and Sample Preparation**

The liver, kidneys, lungs, and spleens were harvested and weighed to determine absolute organ weights. Relative organ weight was calculated as follows: relative organ weight (%) = [organ weight (g)/maternal body weight (g)] × 100. Following subsequent biochemical analysis, each organ was minced into small pieces and homogenized in cold 1.15% potassium chloride (KCl) (Cat. No. P4504; Sigma-Aldrich) to prepare 10% (w/v) tissue homogenates using an Ultra-Turrax T25 homogenizer (IKA-Werke GmbH & Co. KG, Staufen, Germany), as previously described (15), but with modifications. The homogenates were centrifuged at 10,000 rpm for 15 min at 4°C using a refrigerated centrifuge Mikro 200R (Hettich Zentrifugen, Manchester, UK). The supernatants were collected, aliquoted, and stored at -80°C until biochemical analyses. Figure 1 illustrates the experimental design and sample preparation workflow.

**Protein Determination**

Protein content was determined using the Bradford method as previously described.(16) A standard curve was prepared by serial dilution of a 2 mg/mL bovine serum albumin (BSA) (Cat. No. A2153; Sigma-Aldrich) stock solution. Briefly, 5 µL of each tissue homogenate or BSA standard was added to a 96-well microplate in triplicate, followed by 250 µL of Bradford reagent prepared using Coomassie Brilliant Blue G-250 (Cat. No. B0770; Sigma-Aldrich). The mixture was incubated in the dark at room temperature for 5 min. Absorbance was measured at 595 nm using a VersaMax ELISA Microplate Reader (Molecular Devices, San Jose, CA, USA), and protein concentrations were determined against the BSA standard curve.

**Assessment of Oxidative Stress**

Malondialdehyde (MDA) levels were determined based on the reaction of MDA with thiobarbituric acid (TBA) under acidic, high-temperature conditions to form a thiobarbituric acid-reactive substances (TBARS) chromophore.(17) An MDA standard curve (0-40.5 nmol/L) was prepared using 1,1,3,3-tetraethoxypropane (TEP) (Cat. No. T9889; Sigma-Aldrich). Briefly, 50 µL of tissue homogenate was mixed with 250 µL of 19.93% trichloroacetic acid (TCA) (Cat. No. T9159; Sigma-Aldrich) prepared in 0.06 M hydrochloric acid (HCl) (Cat. No. 258148; Sigma-Aldrich). Following incubation in the dark for 15 min, 150 µL of 0.67% 2-TBA (Cat. No. T5500; Sigma-Aldrich), prepared in 0.05 M sodium hydroxide (NaOH) (Cat. No. 221465; Sigma-Aldrich), was added. The reaction mixture was heated at 100°C for 30 min to precipitate proteins and remove excess reagents, then cooled to room temperature. Following centrifugation at 3,000 rpm for 10 min, 200 µL of the supernatant was transferred to a 96-well microplate. Absorbance was measured at 532 nm using a VersaMax

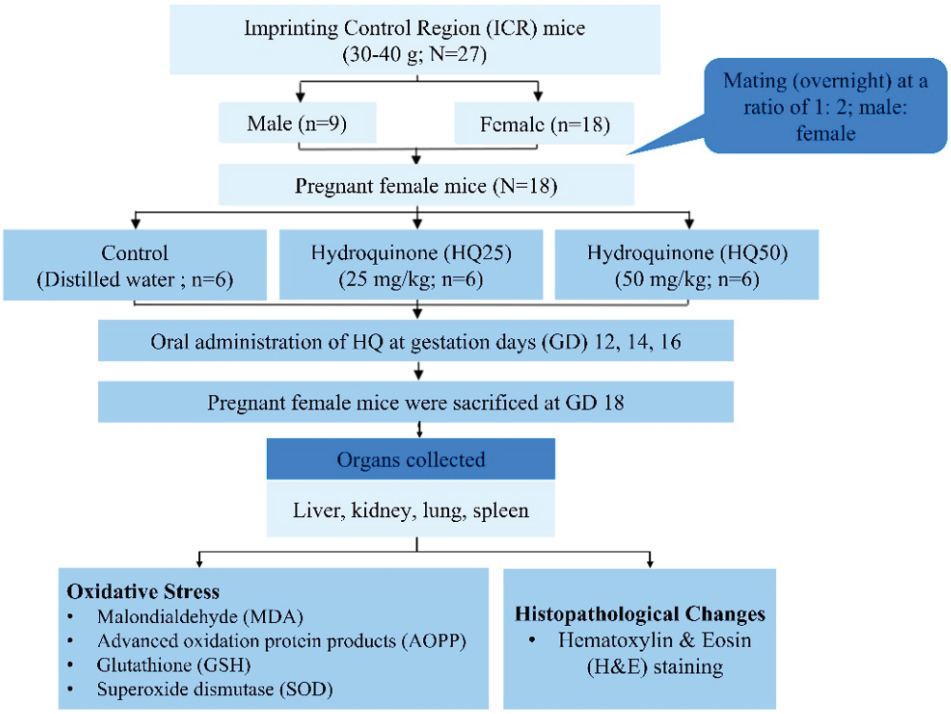



**Figure 1. An overview of the experimental design and sample preparation workflow.**

ELISA Microplate Reader (Molecular Devices), and MDA concentrations were determined against the standard curve. Advanced oxidation protein products (AOPP) were quantified according to the oxidation of iodide ($I^-$) by oxidized protein products under acidic conditions, yielding a chromophore according to the previously described method.(18) A standard curve (0-500 µmol/L) was prepared using chloramine-T trihydrate (Cat. No. 402869; Sigma-Aldrich). Briefly, 200 µL of tissue homogenate supernatant was added to a 96-well microplate, followed by 10 µL of 1.16 M potassium iodide (KI) (Cat. No. 207969; Sigma-Aldrich). Following incubation for 2-5 min, 20 µL of 50% acetic acid (Cat. No. 695092; Sigma-Aldrich) was added to terminate the reaction. After a further 30 s, absorbance was measured at 340 nm using a VersaMax ELISA Microplate Reader (Molecular Devices). AOPP levels were determined against the chloramine-T standard curve and expressed as µmol/g protein.

**Assessment of Antioxidant Status**

Glutathione (GSH) levels were assessed through oxidation with 5,5′-dithiobis(2-nitrobenzoic acid) (DTNB), which reacts with sulfhydryl groups to produce a chromophore. (19) Phosphate buffers were prepared using disodium hydrogen phosphate ($Na_2HPO_4$) (Cat. No. S9763; Sigma-Aldrich) and ethylenediaminetetraacetic acid disodium salt dihydrate (EDTA) (Cat. No. E5134; Sigma-Aldrich). A GSH standard curve was prepared from a 10 mM reduced glutathione stock solution (Cat. No. G4251; Sigma-Aldrich). For sample analysis, 50 µL of tissue homogenate was mixed with 40 µL of phosphate buffer (pH 8.0) and 10 µL of DTNB (Cat. No. D8130; Sigma-Aldrich). The reaction mixture was incubated at room temperature for 15 min, and absorbance was measured at 415 nm using a VersaMax ELISA Microplate Reader (Molecular Devices). GSH levels were determined against the standard curve.

Superoxide dismutase (SOD) activity was quantified by measuring its capacity to suppress the superoxide radical-mediated reduction of nitroblue tetrazolium (NBT) with reduction of NBT generates a blue formazan product.(20) The reaction substrate was prepared using 50 mM phosphate buffer (pH 7.8) containing disodium hydrogen phosphate ($Na_2HPO_4$) (Cat. No. S9763; Sigma-Aldrich), sodium dihydrogen phosphate monohydrate ($NaH_2PO_4 \cdot H_2O$) (Cat. No. 106349; Merck, Darmstadt, Germany), EDTA (Cat. No. E5134; Sigma-Aldrich), 30 mg/mL L-methionine (Cat. No. 166160250; Acros Organics, Geel, Belgium), 1.40 mg/mL NBT (Cat. No. N6876; Sigma-Aldrich), and 1% Triton X-100 (Cat. No. X100; Sigma-Aldrich). Briefly, 1.0 mL of the substrate mixture was mixed with 20 µL of tissue supernatant and 10 µL of 0.44 mg/mL riboflavin (Cat. No. 132350250; Acros Organics). The reaction mixture was exposed to two 18-W fluorescent lamps for 7 min, and absorbance was measured at 560 nm using ELISA microplate reader. SOD activity was normalized to protein content and expressed as E/mg protein/min.

### Histopathological Study

The liver, kidneys, lungs, and spleen were excised and immediately fixed in 10% neutral buffered formalin (Cat. No. HT501128; Sigma-Aldrich) to preserve tissue morphology and architecture. The fixed tissues were subsequently processed using an automated Leica tissue processor Leica TP1020 (Leica, Wetzlar, Germany), involving graded ethanol dehydration (Cat. No. 100983; Merck), xylene clearing (Cat. No. 534056; Sigma-Aldrich), and paraffin wax infiltration (Cat. No. 76233; Sigma-Aldrich). The processed tissues were embedded in paraffin using an embedding machine Leica EG1160 (Leica). Then, the sections measuring 3-5 µm in thickness were prepared using a rotary microtome Leica RM2135 (Leica). The sections were mounted on glass slides and stained with hematoxylin and eosin (H&E) followed by cover-slipping with distyrene-plasticizer-xylene (DPX) mounting medium. Histopathological evaluation was conducted qualitatively by light microscopy Nikon Eclipse 80i (Nikon Corporation, Tokyo, Japan) based on the method described.(21) Cellular morphology, tissue organization, and structural integrity were qualitatively assessed across the examined organs in accordance with established principles for the assessment and reporting of pathological changes in animal tissues.(22) Representative digital photomicrographs were captured at 10× and 40× magnifications using a MicroPublisher 5.0 RTV camera (QImaging, Surrey, Canada) to record histopathological alterations, including cellular necrosis, vascular congestion, and inflammatory cell infiltration.

### Statistical Analysis

All quantitative data were analyzed using the Statistical Package for the Social Sciences (SPSS) version 26.0 (IBM Corporation, Armonk, NY, USA). Normality was assessed using the Shapiro-Wilk test. Given the small sample size (n=6 per group), the results of the normality assessment were interpreted cautiously. Homogeneity of variances was assessed using Levene's test. For data satisfying the assumptions of normality and homogeneity of variance, differences among the control, HQ25, and HQ50 groups were analyzed using one-way analysis of variance (ANOVA), followed by Tukey's post hoc test for pairwise comparisons. Data are expressed as mean±standard error of the mean (SEM). Statistical significance was defined as $p<0.05$.

## Results

### Selective Alterations of Maternal Physiological Parameters Following HQ Exposure

As shown in Table 1, significant differences ($p<0.05$) in maternal body weight gain and food intake were observed only in the HQ50 group compared with the control group, whereas no significant difference ($p>0.05$) in water intake was observed among the groups. No mortality or overt signs of morbidity were observed in any experimental group throughout the study period. Individual maternal body weights at selected gestational time points (GD-0, -12, -14, -16, and -18) were provided in Supplementary Table S1. The time points were selected based on the onset of HQ exposure, which is initiated at GD-12.

### Gestational HQ Exposure Showed No Significant Effect on Maternal Organ Weights

The comparison of corresponding organ weight data between groups were presented in Table 2. Absolute and relative weights of the liver, kidney, lung, and spleen showed no statistically significant ($p>0.05$) differences among the control, HQ25, and HQ50 groups.

**Table 1. Maternal body weight gain, food and water intake, mortality and morbidity percentages following HQ exposure.**

| Organs | Groups | | | *p* -value |
|---|---|---|---|---|
| | Control (n=6) | HQ25 (n=6) | HQ50 (n=6) | |
| Body weight gain (g), mean±SEM | 34.51±1.91 | 29.65±2.08 | 24.27±0.49* | 0.01 |
| Food intake (g), mean±SEM | 84.09±0.97 | 80.15±2.25 | 75.20±1.91* | 0.02 |
| Water intake (mL), mean±SEM | 247.97±3.14 | 239.23±5.28 | 235.17±3.37 | 0.17 |
| Mortality, n (%) | 0 (0) | 0 (0) | 0 (0) | - |
| Overt signs of morbidity, n (%) | 0 (0) | 0 (0) | 0 (0) | - |

Statistical comparisons of maternal body weight gain, food intake, and water intake among groups were performed using one-way ANOVA followed by Tukey's post hoc test. *$p<0.05$ vs. the control group.

**Table 2. Absolute and relative organ weights of maternal mice following HQ exposure.**

| Parameters | Organs | Groups | | | *p*-value |
|---|---|---|---|---|---|
| | | Control (n=6) | HQ25 (n=6) | HQ50 (n=6) | |
| Absolute weight (g) | Liver | 3.02± 0.11 | 2.78±0.12 | 2.91±0.19 | 0.51 |
| | Kidney | 0.24±0.01 | 0.23±0.01 | 0.24±0.01 | 0.97 |
| | Lung | 0.11±0.01 | 0.13±0.01 | 0.13±0.01 | 0.54 |
| | Spleen | 0.19±0.02 | 0.16±0.01 | 0.18±0.01 | 0.20 |
| Relative weight (%) | Liver | 5.42±0.39 | 4.83±0.34 | 4.62±0.35 | 0.30 |
| | Kidney | 0.42±0.02 | 0.41±0.03 | 0.37±0.02 | 0.39 |
| | Lung | 0.20±0.03 | 0.22±0.02 | 0.20±0.02 | 0.69 |
| | Spleen | 0.34±0.04 | 0.28±0.02 | 0.29±0.01 | 0.19 |

Data are presented as mean±SEM. Statistical comparisons of absolute and relative organ weights among groups were performed using One-way ANOVA followed by Tukey's post hoc test.

**Limited Alterations in Organ-Specific Oxidative Stress Markers following HQ Exposure**

Table 3 showed the MDA and AOPP levels following HQ exposure across the examined maternal organs. No statistically significant differences in MDA or AOPP levels were observed between the control and HQ-treated groups in any of the organs evaluated ($p>0.05$). Overall, MDA and AOPP levels remained comparable across the control and HQ-treated groups, suggesting that gestational HQ exposure did not produce detectable changes in these markers of lipid and protein oxidation under the experimental conditions.

**Reduced Splenic GSH and Pulmonary SOD Activity following HQ Exposure**

Table 4 presented the GSH levels and SOD activities following HQ exposure across the examined maternal organs. No statistically significant differences in GSH levels were observed between the control and HQ-treated groups in the liver, kidney, or lung, although a decreasing trend was observed in all three organs. In contrast, GSH levels were significantly reduced in the spleen following exposure to 50 mg/kg HQ compared with the control group ($p<0.05$), whereas the reduction observed at 25 mg/kg was not statistically significant. Similarly, SOD activity did not differ significantly between the control and HQ-treated groups in the liver, kidney, or spleen. However, in the lung, SOD activity was significantly lower in both the HQ25 and HQ50 groups compared with the control group ($p<0.05$).

**Multi-Organ Cellular Injury and Tissue Structural Alterations following HQ Exposure**

Histopathological changes in the examined maternal organs following in utero HQ exposure were presented in Figures 2-5. Representative sections were examined at 10× and

**Table 3. Oxidative stress profiles of maternal organs following exposure to HQ.**

| Parameters | Organs | Groups | | | *p*-value |
|---|---|---|---|---|---|
| | | Control (n=6) | HQ25 (n=6) | HQ50 (n=6) | |
| MDA (nmol/g protein) | Liver | 5.69±1.28 | 7.83±1.17 | 6.73±0.83 | 0.46 |
| | Kidney | 65.91±10.90 | 55.34±8.98 | 43.02±3.16 | 0.19 |
| | Lung | 40.53±6.35 | 41.45±5.47 | 44.49±5.29 | 0.53 |
| | Spleen | 30.60±4.57 | 38.80±3.50 | 44.86±7.30 | 0.24 |
| AOPP (µmol/g protein) | Liver | 243.47±3.85 | 259.06±3.83 | 251.35±3.93 | 0.08 |
| | Kidney | 162.38±18.13 | 117.39±15.58 | 107.78±12.97 | 0.06 |
| | Lung | 23.32±3.72 | 31.43±2.72 | 36.15±5.54 | 0.12 |
| | Spleen | 155.68±15.09 | 239.12±46.70 | 216.58±31.09 | 0.28 |

Data are presented as mean±SEM. Statistical comparisons among groups were performed using One-way ANOVA followed by Tukey's post hoc test.

**Table 4. Antioxidant status of maternal organs following exposure to HQ.**

| Parameters | Organs | Groups | | | *p*-value |
|---|---|---|---|---|---|
| | | Control (n=6) | HQ25 (n=6) | HQ50 (n=6) | |
| GSH (mmol/g protein) | Liver | 0.57±0.09 | 0.47±0.10 | 0.43±0.06 | 0.51 |
| | Kidney | 0.46±0.06 | 0.41±0.04 | 0.37±0.03 | 0.34 |
| | Lung | 1.23±0.11 | 1.26±0.32 | 1.64±0.50 | 0.67 |
| | Spleen | 0.60±0.03 | 0.53±0.02 | 0.46±0.04* | 0.02 |
| SOD (U/min/mg protein) | Liver | 1.89±0.20 | 1.79±0.16 | 1.55±0.17 | 0.40 |
| | Kidney | 4.43±0.67 | 2.45±0.68 | 2.61±0.70 | 0.11 |
| | Lung | 8.72±0.97 | 2.51±0.34* | 3.10±0.32* | 0.01 |
| | Spleen | 3.22±0.29 | 2.73±0.46 | 1.91±0.423 | 0.10 |

Data are presented as mean±SEM. Statistical analysis was performed using One-way ANOVA followed by Tukey's post hoc test. *$p$<0.05 *vs.* the control group.

40× magnifications. In the liver (Figure 2), the control group exhibited preserved hepatic architecture and intact hepatocytes as observed at 10× magnification. At higher magnification, the control group showed a distinct central vein containing erythrocytes within the lumen, well-defined hepatic sinusoids, and identifiable Kupffer cells. In contrast, both HQ-treated groups exhibited alterations in hepatic morphology, including disruption of normal hepatic lobular architecture, hepatocellular necrosis, and central venous congestion, characterized by increased accumulation of blood within the vascular lumen.

Meanwhile, in kidney (Figure 3), the histopathological assessment at 10× magnification revealed that the control group exhibited normal renal architecture, characterized by well-defined glomeruli surrounded by Bowman's capsules and clearly visible Bowman's spaces. At higher magnification, the control group showed intact proximal and distal convoluted tubules, with proximal tubular epithelial cells displaying a cuboidal morphology and prominent microvilli. In contrast, both HQ25 and HQ50 exhibited histopathological alterations compared with the control group, including reduced Bowman's space,

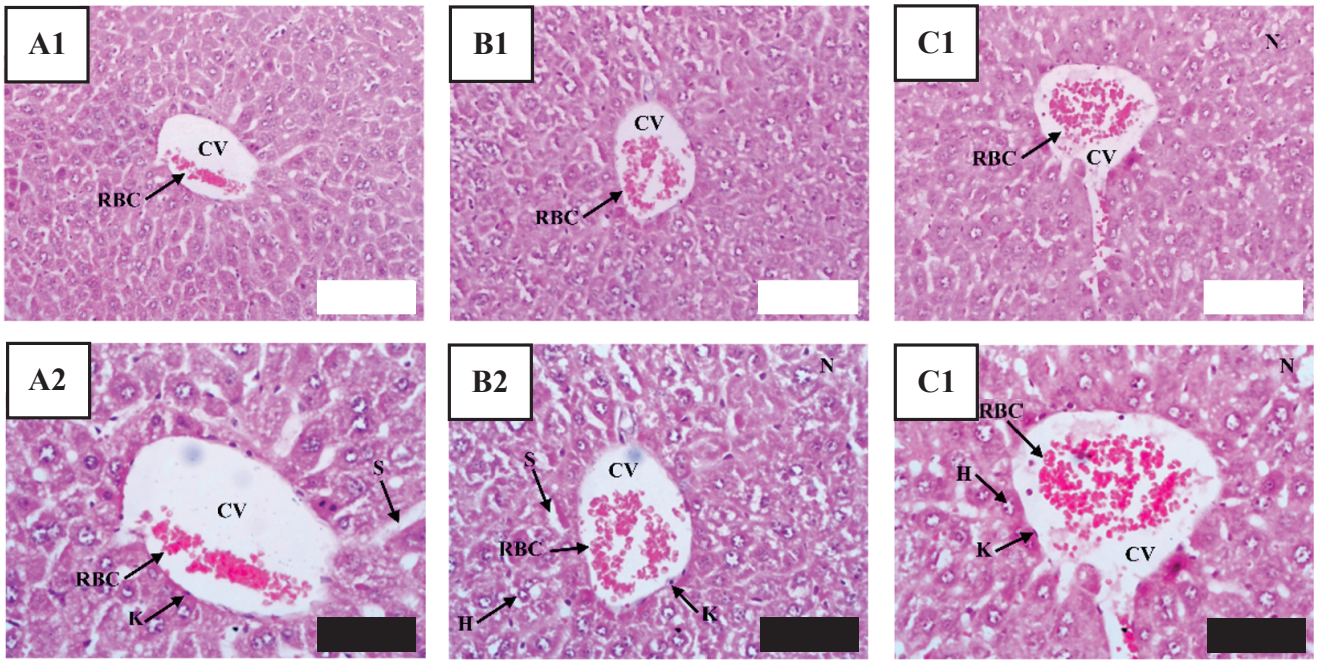



**Figure 2. Histopathological assessment of the liver in maternal mice induced by HQ.** A: Control group; B: HQ25 group; C: HQ50 group. White bar: 200 µm; Black bar: 50 µm. H: Hepatocyte cell, CV: Central vein, RBC: Red blood cell, S: Sinusoidal projections, K: Kupffer cells, N: Necrotic hepatocytes.

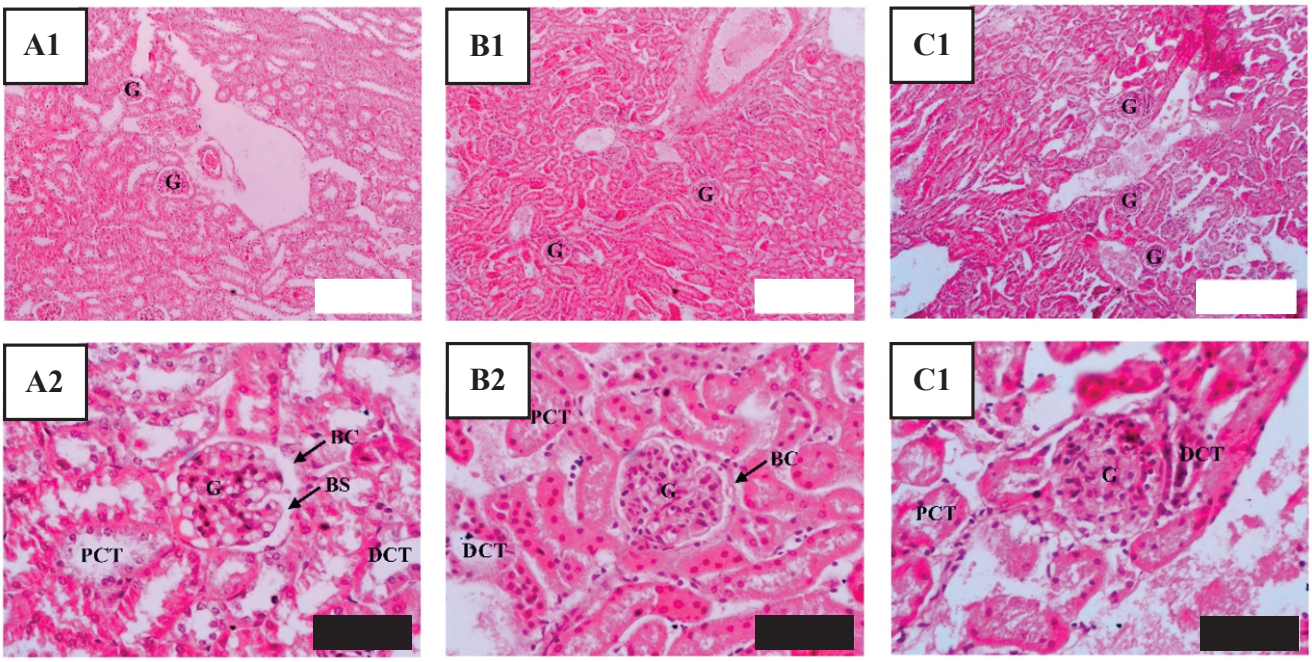



**Figure 3. Histopathological assessment of the kidney in maternal mice induced by HQ.** A: Control group; B: HQ25 group; C: HQ50 group. White bar: 200 µm; Black bar: 50 µm. G: Glomerulus, BC: Bowman's capsule, BS: Bowman's space, PCT: Proximal convoluted tubule, DCT: Distal convoluted tubule.

increased glomerular cellularity, and thickening of the glomerular basement membrane. Additional morphological alterations were observed in the HQ50 group, including glomerular shrinkage, increased Bowman's capsule, tubular degeneration, and degeneration of the proximal convoluted tubules accompanied by loss of microvilli.

As shown in Figure 4, lung tissues from the control group exhibited normal histological architecture, characterized by intact blood vessels, bronchioles, and alveolar structures. In contrast, both HQ-treated groups demonstrated histopathological alterations, including irregular bronchial walls, inflammatory cell infiltration,

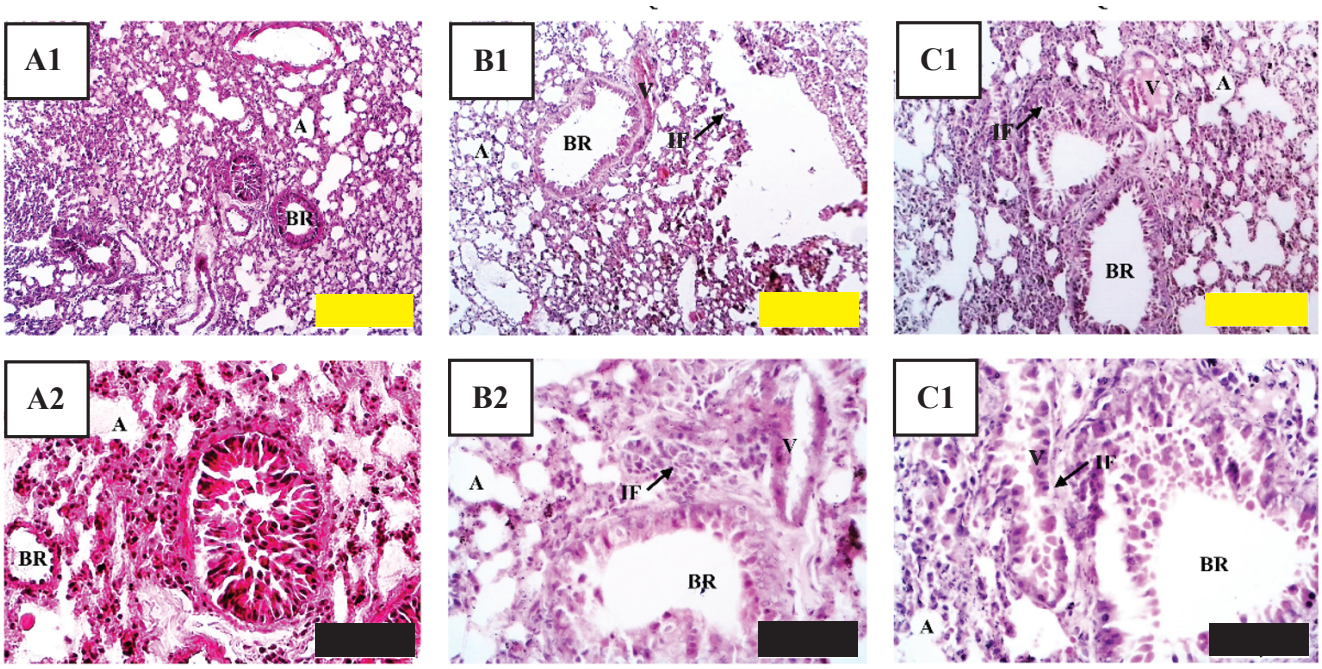



**Figure 4. Histopathological assessment of the lung in maternal mice induced by HQ.** A: Control group; B: HQ25 group; C: HQ50 group. Yellow bar: 200 µm; Black bar: 50 µm. V: Blood vessel, BR: Bronchioles, A: Alveolar, IF: Inflammatory cell infiltration.

enlarged alveolar spaces, and degeneration of the bronchial epithelial lining.

In the spleen (Figure 5), the control group exhibited preserved splenic architecture, with distinct white and red pulp compartments. The white pulp contained central arterioles and germinal centres surrounded by lymphoid follicles. Meanwhile, both HQ25 and HQ50 exhibited altered splenic histological features, characterized by increased cellularity within the red pulp, increased lymphocytic aggregation within the white pulp, and inflammatory cell infiltration.

## Discussion

Benzene is a volatile organic compound extensively used in industrial applications. HQ, a major metabolite of benzene, undergoes myeloperoxidase (MPO)-mediated oxidation and autoxidation, generating reactive semiquinone intermediates that contribute to quinone-mediated toxicity.(1) In the current study, pregnant mice were orally administered HQ at the doses of 25 and 50 mg/kg on GD-12, -14, and -16, based on previously established experimental models.(13,23) The higher dose was adapted from previous study (13), while the lower dose was included to evaluate dose-dependent effects. This approach aligns with toxicological principles emphasizing evaluation across exposure ranges.(24) These doses represent experimental toxicological exposures rather than direct equivalents of typical human occupational exposure. For context, the National Institute of Occupational Safety and Health (NIOSH) (recommended exposure limit (REL) for HQ is 2 mg/m³ as a 15-min ceiling.(25) However, direct quantitative comparison with the doses used in the present study is not appropriate because of differences in exposure route, duration, and exposure pattern. Given that pregnancy involves substantial physiological and metabolic adaptations that may heighten susceptibility to toxicants, assessing the impact of HQ on maternal health and organ systems is critical.

Oxidative stress biomarkers showed numerical variations following HQ exposure, although most changes did not reach statistical significance. MDA, a secondary product of lipid peroxidation, was higher across several organs in HQ-treated groups; however, these differences were not statistically significant and therefore do not provide conclusive evidence of enhanced lipid peroxidation. Elevated MDA has previously been reported in L02 hepatocytes following HQ exposure (26), in kidneys of benzene-exposed rats (27), and in rats exposed to benzene vapour.(28) However, these studies involved *in vitro*, non-gestational, or different exposure routes and models; therefore, direct comparison with the present gestational oral-exposure model should be made cautiously. Benzene metabolism generates reactive intermediates that enhance ROS production (5), and oxidative stress occurs when ROS

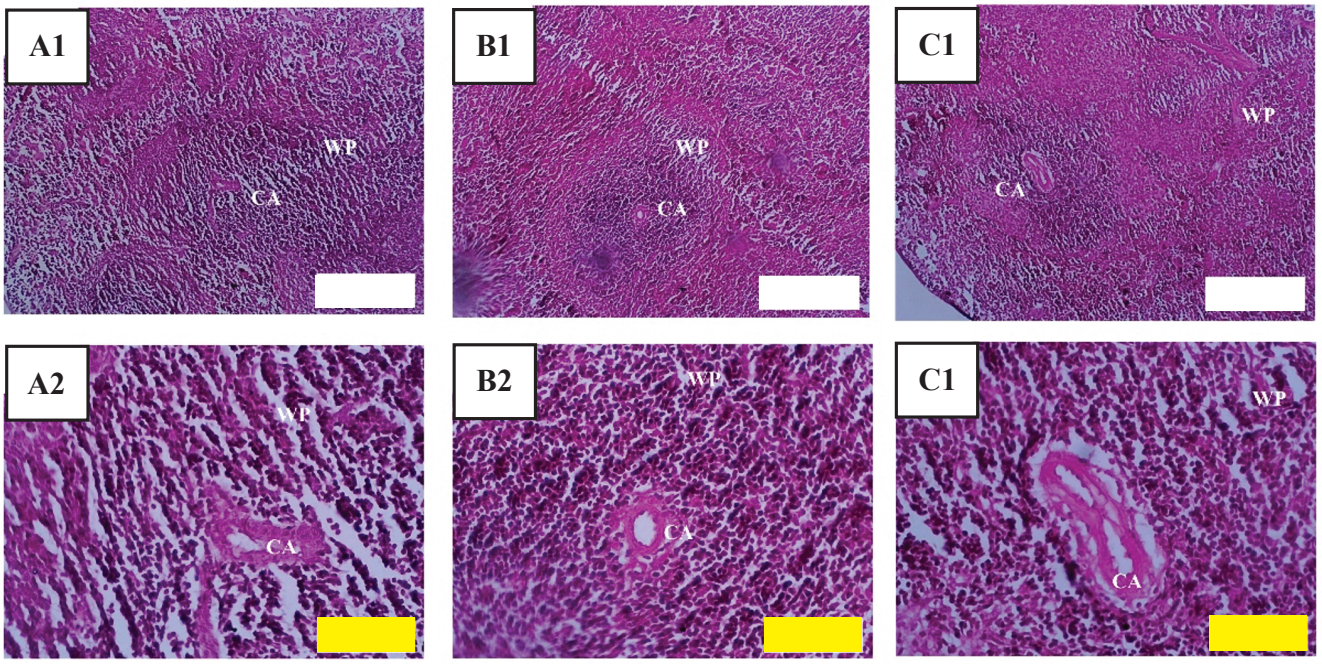



**Figure 5. Histopathological assessment of the spleen in maternal mice induced by HQ.** A: Control group; B: HQ25 group; C: HQ50 group. White bar: 200 µm; Yellow bar: 50 µm. WP: White pulp, CA: Central artery.

generation exceeds antioxidant capacity, damaging lipids, proteins, and DNA.(5) Lipids are particularly vulnerable due to their double bonds, with MDA formed during polyunsaturated fatty acid (PUFA) peroxidation.(29) MDA can further react with DNA and proteins, contributing to biomolecular dysfunction.(29) Although these mechanisms provide a biological basis for lipid peroxidation, the non-significant MDA changes observed in the present study do not establish increased oxidative damage following gestational HQ exposure.

Protein oxidation was assessed via AOPP, which consists of oxidatively modified, cross-linked proteins containing tyrosine residues.(30) Although increases in AOPP were observed in some HQ-treated groups, these differences were not statistically significant. Similar observations of protein oxidation have been reported in gasoline station workers exposed to benzene (31) and in rats administered bromobenzene.(32) However, these studies differ from the present investigation in terms of exposure conditions, chemical exposure, and experimental population, limiting direct mechanistic comparison. Proteins rich in unsaturated bonds and sulfur-containing amino acids are particularly susceptible to ROS-mediated oxidation, impairing structure and function.(30) AOPP, considered a uremic toxin, may also activate mononuclear phagocytes via the $H_2O_2$-MPO pathway.(30) Nevertheless, the absence of significant AOPP changes in the present study does not provide conclusive evidence of increased protein oxidation.

Antioxidant defences showed organ-specific alterations. GSH, a major endogenous antioxidant, showed numerical reductions in the liver, kidney, and lung, whereas a significant reduction was detected in the spleen. This indicates an alteration in splenic antioxidant defence following HQ exposure. Similar reductions in GSH have been reported in hydrocarbon-exposed kidneys (33) and in cigarette smoke-exposed lungs.(34) HQ can conjugate with GSH, depleting reserves and impairing detoxification.(5) SOD activity also declined, with a significant reduction in lung tissue. This finding is consistent with reduced SOD activity in benzene-exposed workers (35) and mice (36). Although these previous studies provide relevant mechanistic context, differences in exposure route, toxicant, and the use of non-gestational models should be considered when comparing them with the present gestational HQ exposure model. Together, these results indicate organ-specific antioxidant alterations, particularly in the spleen and lung, rather than a generalized oxidative response across maternal organs.

Histopathology outcomes confirmed hepatocellular necrosis and vascular congestion, demonstrating hepatic morphological injury following HQ exposure. These morphological changes mirror those reported in benzene-induced hepatotoxicity.(37) However, differences in exposure route and experimental model limit direct comparison with the present gestational HQ exposure model. Renal histopathology revealed enlarged glomeruli, reduced Bowman's space, increased cellularity, thickened capsules, tubular degeneration, and microvilli loss. Such alterations implicate both glomerular and tubular compartments in HQ-induced injury. Similar findings have been reported in benzene-exposed kidneys (38), although the different exposure conditions and non-gestational models should be considered when drawing mechanistic parallels. Previous evidence suggests that metabolite accumulation in lipid-rich, perfused tissues may contribute to tissue susceptibility.(38)

Pulmonary changes were pronounced: HQ-treated lungs exhibited irregular bronchial walls, enlarged alveolar spaces, bronchiolar dilation, and inflammatory infiltration. Combined with the significant reduction in SOD activity, these findings indicate pulmonary morphological injury accompanied by altered antioxidant defence. Comparisons with cigarette smoke exposure models (39) provide contextual evidence for the involvement of oxidative processes in pulmonary injury; however, differences in toxicant composition, exposure route, and experimental model limit direct mechanistic comparison with gestational HQ exposure. Splenic alterations included increased cellularity in red pulp and lymphocyte accumulation in white pulp, suggesting an adaptive immune response. Unlike benzene-induced splenitis and fibrosis (37), these changes may reflect species or exposure differences. As the spleen regulates both cellular and humoral immunity, lymphocyte accumulation may represent an adaptive response to enhance toxin clearance (40), though functional consequences require further immunological assessment.

Despite these findings, several limitations should be considered. Validation in a larger cohort would strengthen the robustness and generalizability of the findings. Histopathological alterations were assessed qualitatively without quantitative or semi-quantitative scoring, limiting objective comparisons of lesion severity. In addition, fetal and placental endpoints were not quantitatively evaluated; therefore, whether the observed maternal tissue alterations have implications for fetal development remains unclear. Although absolute and relative maternal organ weights were evaluated, mechanistic biomarkers, including

the nuclear factor erythroid 2-related factor 2/heme oxygenase-1 (Nrf2/HO-1) pathway and DNA damage markers, were not investigated. Nevertheless, the present findings provide baseline data on maternal multi-organ responses to gestational HQ exposure. Future studies integrating quantitative histopathological assessment, mechanistic biomarkers, and maternal, placental, as well as fetal endpoints are warranted to provide better understanding with regards to the consequences of gestational HQ exposure.

## Conclusion

In conclusion, gestational HQ exposure induced organ-specific antioxidant alterations and broader histopathological injury across maternal organs. Significant reductions in pulmonary SOD activity and splenic GSH levels indicate differential antioxidant responses, while the absence of significant changes in the other measured oxidative stress markers suggests that oxidative damage was not uniformly evident across organs. Nevertheless, histopathological alterations in the liver, kidney, lung, and spleen demonstrate broader tissue-level injury following HQ exposure. These findings provide baseline data on maternal tissue responses to gestational HQ exposure.

## Acknowledgments

This work was supported by the Fundamental Research Grant Scheme (FRGS) from the Ministry of Higher Education (MOHE), Malaysia (Grant Number: FRGS/1/2021/SKK06/UKM/03/1). The authors would like to thank the lecturers, researchers, and staff of the Biomedical Science Programme, Centre for Diagnostic, Therapeutic and Investigative Studies, Faculty of Health Sciences, Universiti Kebangsaan Malaysia (UKM) for their support and assistance throughout this research. The authors also extend their appreciation to all individuals who contributed directly or indirectly to the completion of this study.

## Authors Contribution

NAY was the main writer and contributed to the manuscript from start to finish, including conceptualizing, writing, and revising the manuscript. ZAH, as the main supervisor, guided the conceptualization of the study, assisted with manuscript editing, and contributed to manuscript corrections. ISI, NAM, NHKZ and SEDA were responsible for data collection and interpreting the data. ZAH, SBB, IST, NNMA and NMAW contributed to reviewing, correcting, and ensuring the manuscript flow before submission. All authors contributed to the critical revision, approved the final manuscript, and take responsibility for the integrity of the data.

## Ethical Statement

All experimental procedures were conducted at the Animal House, Kuala Lumpur, Malaysia, following approval by the Animal Ethics Committee of Universiti Kebangsaan Malaysia (UKMAEC), under Ethics Number: FSK/2022/ZARIYANTEY/23-MAC/1237-MAC-2022-FEB-2025.

## Conflict of Interest

The authors declare that they have no competing interests.

## References

1. Kumari P, Soni D, Aggarwal SG. Benzene: A critical review on measurement methodology, certified reference material, exposure limits with its impact on human health and mitigation strategies. Environ Anal Health Toxicol. 2024; 39(2): e2024012-0. doi: 10.5620/eaht.2024012.
2. Loomis D, Guyton KZ, Grosse Y, El Ghissassi F, Bouvard V, Benbrahim-Tallaa L, *et al.* International Agency for Research on Cancer Monograph Working Group. Carcinogenicity of benzene. Lancet Oncol. 2017; 18(12): 1574-5.
3. Holmes TH, Winn LM. DNA damage, DNA repair gene expression, and topoisomerase IIα activity in CD-1 mice following in utero benzene exposure. Toxicol Lett. 2022; 368: 47-55.
4. Lu PCW, Shahbaz S, Winn LM. Benzene and its effects on cell signaling pathways related to hematopoiesis and leukemia. J Appl Toxicol. 2020; 40(8): 1018-32.
5. Yusoff NA, Abd Hamid Z, Budin SB, Taib IS. Linking benzene, in utero carcinogenicity and fetal hematopoietic stem cell niches: a mechanistic review. Int J Mol Sci. 2023; 24(7): 6335. doi: 10.3390/ijms24076335.
6. Ibrahim A, Khoo MI, Ismail EHE, Hussain NHN, Zin AAM, Noordin L, *et al*. Oxidative stress biomarkers in pregnancy: A systematic review. Reprod Biol Endocrinol. 2024; 22(1): 93. doi: 10.1186/s12958-024-01259-x.
7. Suryawan A, Rahardjo TM. The role of free radicals and antioxidant in abortion. Indones Biomed J. 2013; 5(1): 25-30.
8. Jia X, Zhu L, Zhu Q, Zhang J. The role of mitochondrial dysfunction in kidney injury and disease. Autoimmun Rev. 2024; 23(6) :103576.

doi: 10.1016/j.autrev.2024.103576.
9. Grant T, Brigham EP, McCormack MC. Childhood origins of adult lung disease as opportunities for prevention. J Allergy Clin Immunol Pract. 2020; 8(3): 849-8.
10. Schnatter AR, Rooseboom M, Kocabas NA, North CM, Dalzell A, Twisk J, *et al.* Derivation of an occupational exposure limit for benzene using epidemiological study quality assessment tools. Toxicol Lett. 2020; 334: 117-44.
11. Yusoff NA, Taib IS, Budin SB, Mohamed M. Paternal fenitrothion exposures in rats causes sperm DNA fragmentation in F0 and histomorphometric changes in selected organs of F1 generation. Toxics. 2021; 9(7): 159. doi: 10.3390/toxics9070159.
12. Arifin WN, Zahiruddin WM. Sample size calculation in animal studies using resource equation approach. Malays J Med Sci. 2017; 24(5): 101-5.
13. Mansell E, Zareian N, Malouf C, Kapeni C, Brown N, Badie C, *et al.* DNA damage signalling from the placenta to foetal blood as a potential mechanism for childhood leukaemia initiation. Sci Rep. 2019; 9(1): 4370. doi: 10.1038/s41598-019-39552-0.
14. Grzeszczak K, Łanocha-Arendarczyk N, Malinowski W, Ziętek P, Kosik-Bogacka D. Oxidative stress in pregnancy. Biomolecules. 2023; 13(12): 1768. doi: 10.3390/biom13121768.
15. Yusoff NA, Juremi II, Budin SB, Taib IS. Repeated administration of fenitrothion alters renal functions via oxidative stress mechanism without inhibiting acetylcholinesterase activity in rats. Life Sci. Med. Biomed. 2020; 4(9): 1-6. doi: 10.28916/lsmb.4.9.2020.70
16. Bradford MM. A rapid and sensitive method for the quantitation of microgram quantities of protein utilizing the principle of protein-dye binding. Anal Biochem. 1976; 72: 248-54.
17. Stocks J, Dormandy TL. The autoxidation of human red cell lipids induced by hydrogen peroxide. Br J Haematol. 1971; 20(1): 95-111.
18. Witko-Sarsat V, Friedlander M, Capeillère-Blandin C, Nguyen-Khoa T, Nguyen AT, Zingraff J, *et al.* Advanced oxidation protein products as a novel marker of oxidative stress in uremia. Kidney Int. 1996; 49(5): 1304-13.
19. Ellman GL. Tissue sulfhydryl groups. Arch Biochem Biophys. 1959; 82(1): 70-7.
20. Beyer WF Jr, Fridovich I. Assaying for superoxide dismutase activity: Some large consequences of minor changes in conditions. Anal Biochem. 1987; 161(2): 559-66.
21. Ochei J, Kolhatkar A. Medical Laboratory Science: Theory and Practice. 1st ed. New Delhi: Tata McGraw-Hill Publishing Company Limited; 2000.
22. Scudamore CL, Soilleux EJ, Karp NA, Smith K, Poulsom R, Herrington CS, *et al.* Recommendations for minimum information for publication of experimental pathology data: MINPEPA guidelines. J Pathol. 2016; 238(2): 359-67.
23. Badham HJ, Winn LM. In utero exposure to benzene disrupts fetal hematopoietic progenitor cell growth via reactive oxygen species. Toxicol Sci. 2010; 113(1): 207-15.
24. Organisation for Economic Co-operation and Development [Internet]. Prenatal Developmental Toxicity Study, Guideline for the Testing of Chemicals (No. 414) [updated 2018 Jun 27; cited 2025 Jul 1]. Available from: https://doi.org/10.1787/9789264070820-en.
25. National Institute for Occupational Safety and Health [Internet]. NIOSH Pocket Guide to Chemical Hazards: Hydroquinone. Centers for Disease Control and Prevention [updated 2019 Oct 30; cited 2026 Sep 29]. Available from: https://www.cdc.gov/niosh/npg/npgd0338.html.
26. Gao Y, Tang H, Xiong L, Zou L, Dai W, Liu H, *et al.* Protective effects of aqueous extracts of Flos lonicerae Japonicae against hydroquinone-induced toxicity in hepatic L02 cells. Oxid Med Cell Longev. 2018; 4: 1-11. doi: 10.1155/2018/4528581.
27. Zeghib K, Boutlelis DA. Protective role of aqueous extract of Atriplex Halimus L. against benzene-induced damage on renal function and glomerular cells in rats. Asian J Pharm Clin Res. 2019; 12(3): 387-92.
28. Cho ES, Kim YS, Choi HY, Rim KT. Effect of inhaled 1,2-dichlorobenzene on cytochrome P450s and lipid peroxidation in B6C3F1 mice. J Biomed Transl Res. 2023; 24(3): 67-82.
29. Fadlilah DN, Izati R, Al Faizah BN, Kavitarna SA, Ardiansyah E, Sa'adah NAM, *et al*. Green tea yoghurt with encapsulated Lacticaseibacillus paracasei E1 improves hepatocyte damage in high-fat high-fructose diet mice by reducing MDA and increasing SOD. Mol Cell Biomed Sci. 2024; 8(3): 185-93.
30. Klobučar I, Hofmann L, Habisch H, Lechleitner M, Klobučar L, Trbušić M, *et al.* Advanced oxidation protein products are strongly associated with the serum levels and lipid contents of lipoprotein subclasses in healthy volunteers and patients with metabolic syndrome. Antioxidants. 2024; 13(3): 339. doi: 10.3390/antiox13030339.
31. Costa C, Ozcagli E, Gangemi S, Schembri F, Giambò F, Androutsopoulos V, *et al*. Molecular biomarkers of oxidative stress and role of dietary factors in gasoline station attendants. Food Chem Toxicol. 2016; 90: 30-5. doi: 10.1016/j.fct.2016.01.017.
32. Ramakrishna V, Gopi S, Setty OH. Protective effect of Phyllanthus fraternus against bromo-benzene-induced mitochondrial dysfunction in rat kidney. Chin J Nat Med. 2013; 10(5): 328-3.
33. Azeez OM, Akhigbe RE, Anigbogu CN. Oxidative status in rat kidney exposed to petroleum hydrocarbons. J Nat Sci Biol Med. 2013; 4(1): 149-54.
34. Gould NS, Min E, Gauthier S, Martin RJ, Day BJ. Lung glutathione adaptive responses to cigarette smoke exposure. Respir Res. 2011; 12(1): 133. doi: 10.1186/1465-9921-12-133.
35. Abdel Maksoud HA, Elharrif MG, Mahfouz MK, Omnia MA, Abdullah MH, Eltabey ME. Biochemical study on occupational inhalation of benzene vapours in petrol station. Respir Med Case Rep. 2019; 27: 100836. doi: 10.1016/j.rmcr.2019.100836.
36. Moarref M, Safavi M, Mostafavi MA, Karami-Mohajeri S. Benzene and erythrocyte aging sub-acute exposure to benzene accelerates the aging process of red blood cells; an in vivo study. Iran J Blood Cancer. 2021; 12(4): 131-7.
37. Kareem DA, Majeed MF, Jasim NH. Ghaji MS. Effect of benzene inhalation on some histological changes in liver, kidney, spleen and pancreas in male mice. Biochem Cell Arch. 2021; 21(2): 3647-52.
38. Kadhim HM, Al-shammari AM, Tawfeeq AT, Mohammad MH, Hassan AA. Benzene histotoxic and teratogenic effects in exposed mice. Kufa Jou Vete Med Sci 2018; 8(2): 1-9. doi: 10.36326/kjvs/2017/v8i24114
39. Ranawat P, Kaur N, Koul A. Modulation of cigarette smoke induced alterations by aqueous Ocimum sanctum leaf extract in pulmonary tissue of rodents. Sci Rep. 2023; 13(1): 15806. doi: 10.1038/s41598-022-26152-8.
40. Wahdaningsih S, Wahyuono S, Riyanto S, Murwanti R. Lymphocyte proliferation and nitric oxide-producing activities of lupeol isolated from red dragon fruit (Hylocereus polyrhizus) extract. Mol Cell Biomed Sci. 2021; 5(1): 8-12.